Supplement of Solid Earth, 7, 1521–1536, 2016
http://www.solid-earth.net/7/1521/2016/
doi:10.5194/se-7-1521-2016-supplement

Solid Earth Open Access EGU

Supplement of

Fully probabilistic seismic source inversion – Part 2: Modelling errors and station covariances

Simon C. Stähler and Karin Sigloch

Correspondence to: Simon C. Stähler (mail@simonstaehler.com)

S1 Resolution power of ℓ^p norms vs D

To demonstrate the results shown in fig. 4 of the main paper (distance between misfit value for true depth compared to noise in sigma) more intuitively, fig. S1 shows perturbed waveforms and the resulting misfit values for a larger set of signal to noise ratios and modelling errors. The figures are otherwise identical to fig. 3 in the paper.

S2 Likelihood distribution parameters

S2.1 μ and σ

To estimate the likelihood distribution of new earthquakes, we need to have an analytical fit function of the distribution parameters $\mu_{\mathrm{P}}, \mu_{\mathrm{SH}}, \sigma_{\mathrm{P}}, \sigma_{\mathrm{SH}}$ in dependence of SNR. Figure S2 shows the parameters with fit functions $h(\mathrm{SNR}) = a_1 + a_2 \cdot \exp(-a_3 \cdot \mathrm{SNR})$. To estimate the goodness of fit, 95% confidence intervals were estimated using the bootstrapping method and added to the figure.

	a_1	a_2	a_3
μ_{P}	-2.06	0.51	0.031
σ_{P}	0.6	-0.093	$2.8 \cdot 10^{-3}$
μ_{SH}	-1.12	0.28	0.24
σ_{SH}	6.7	-6.3	$-0.27 \cdot 10^{-3}$

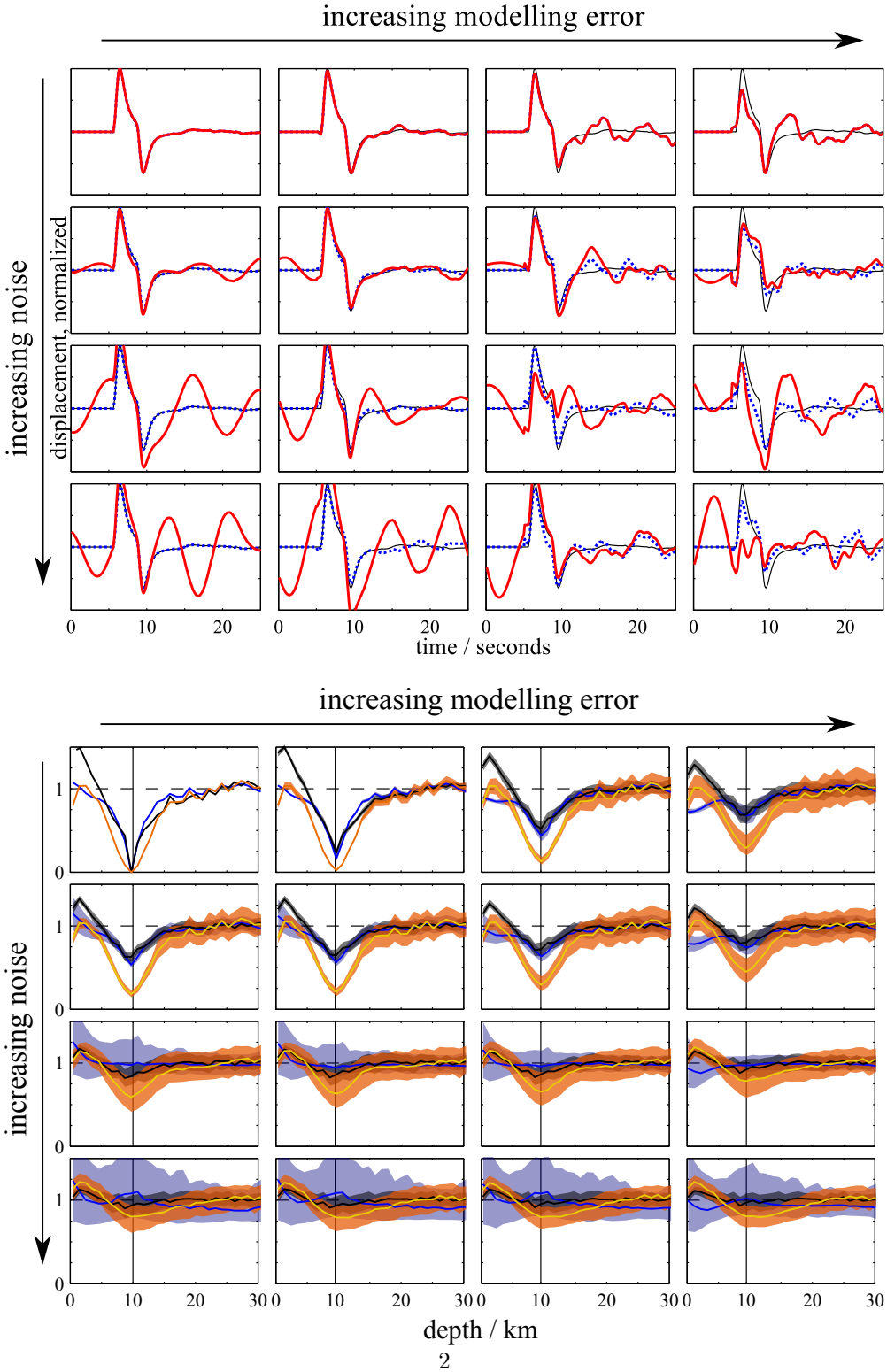

Figure S1: Comparison of the ℓ^1, ℓ^2 norm and the signal decorrelation as misfit criteria in noisy signals, as described in Sect. 2.3 in the main paper. A perturbed synthetic waveform for a 10 km deep earthquake, measured in 40° distance was compared to synthetic seismograms for other depths, using the three misfit criteria. The shaded colours mark the 90% quantiles of the misfit values, calculated by perturbing the reference waveform with different random seeds. The figure shows the relatively high robustness of the cross-correlation coefficient in recognizing reference signals in perturbed measurements. For better visualisation, all misfit values have been normalized separately to have an average values of one between 20 and 30 km.

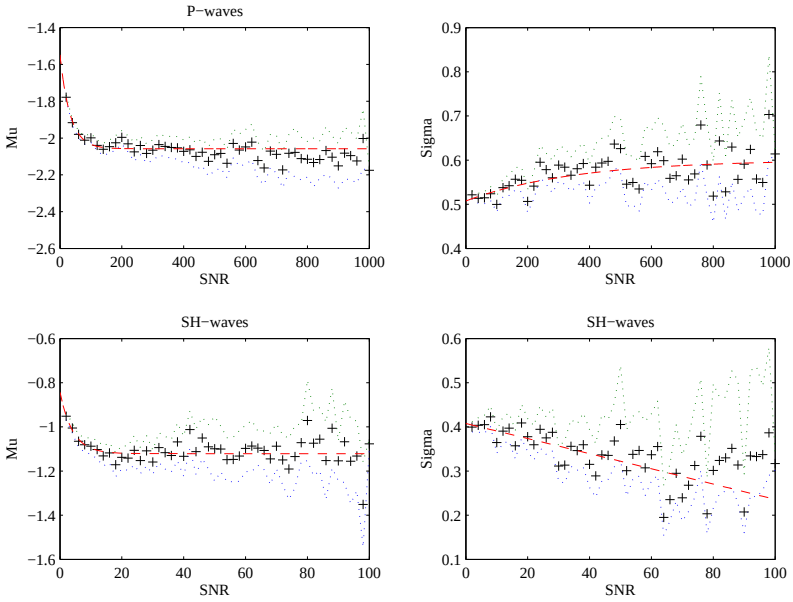

Figure S2: Distribution of parameters μ and σ for P- (top row) and SH-waveforms (bottom row) with respect to the Signal-to-Noise Ratio (SNR). μ_{P} is the expectation value for $\ln(1 - CC_{\max})$ for a waveform with the given SNR, while σ_{P} is the standard deviation. The values in each SNR bin are compared with the fitting function $h(\mathrm{SNR}) = a_1 + a_2 \cdot \exp(-a_3 \cdot \mathrm{SNR})$ (red dashed). Parameters a_1, a_2, a_3 are given in table S2.1. The dotted lines show 95% confidence intervals of the parameters estimated by the bootstrapping method.

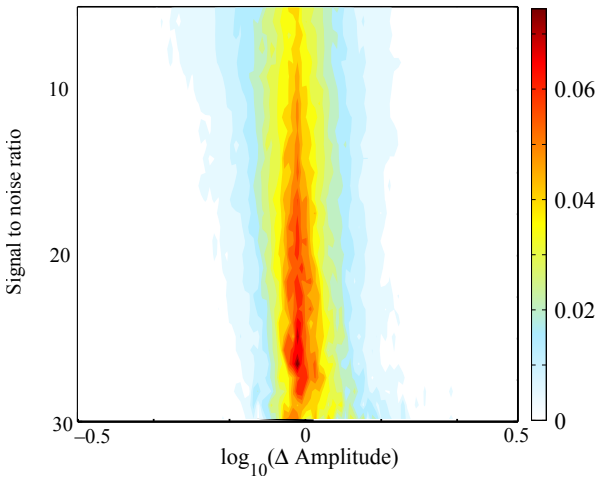

Figure S3: Distribution of amplitude misfits for different signal to noise ratios. Figure is simular to Figure 6 in the paper, but shows the distribution of the amplitude misfit as defined in eq. 28.

S2.2 Amplitudes

The amplitude misfit follows an exponential distribution $|\Delta \log_{10}(A)_j - \text{median}(\Delta \log_{10}(A)_j)| \sim \text{Exp}(\gamma)$, where γ takes the values 0.2 and 0.1 for P and SH respectively. We remove the $\text{median}(\Delta \log_{10}(A)_j)$ before fitting to account for wrongly determined body wave magnitudes in our database. See figure S3 for an overview of the relationship between signal-to-noise ratio and the distribution of $\Delta \log_{10}(A)_j$.

S3 Inter-station correlation

The inter-station correlation was calculated as described in section 3.4 in the paper. To fit it, the function $g(\vartheta) = b_1 + b_2 \cdot \exp(-b_3 \cdot \vartheta^2)$ was used, with the following parameters as a result:

	b_1	b_2	b_3
$r(\vartheta)$	0.049	0.31	$2.17 \cdot 10^{-4}$

The fit function follows the values well (see figure 7 in the paper), although there is a non-explained rise from 160° on. We think that this is an artefact of imperfectly determined focal mechanisms. Stations close to a nodal plane of the radiation pattern will be strongly affected by an error in the strike angle. At the same time, this affects stations at the opposite site of the earthquake, with a back-azimuthmal difference of 180°. Strike-slip events even have a quadrupole radiation pattern, where errors in the strike parameter will influence stations at $0°, 90°, 180°$ and 270°. So, if that explanation was true, there should be another peak at 90°, which is lost here.

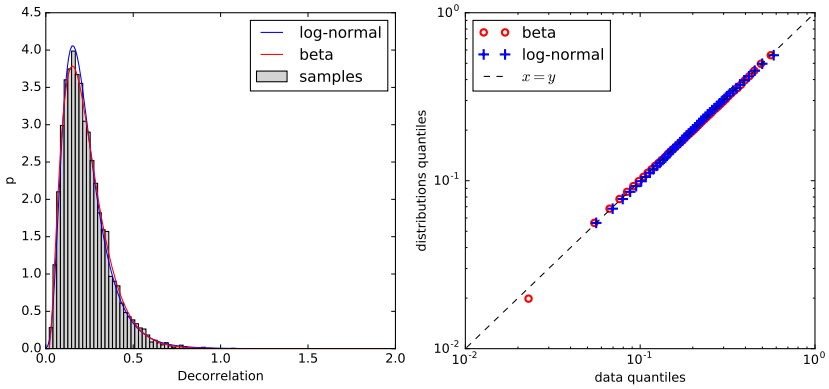

Figure S4: Distribution of decorrelation values between noise-free synthetic data and data perturbed as described in eqs. 17 and 18. (band-limited, "microseismic" noise was added and artificial coda was created by perturbing the phase spectrum). Similar to real data, the values of D are following a log-normal distribution.

S4 Distribution of $D = 1 - CC$ in data with synthetic noise

To test the realism of the synthetic noise and signal perturbations described in sect. 2.4 and eqs. 17 and 18 in the main paper, we tested, whether the distribution of CC values for u_{pert} follows a log-normal distribution as it was found for real data (Fig. 5 in the main paper).